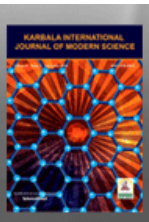

Karbala International Journal of Modern Science

Volume 5 | Issue 3 Article 6

The Improvement of The Solar Air Heater Duct by Wired Ribs Utilization

Osamah Raad Skheel Alkhafaji
Middle Technical University, Baghdad, Iraq, osamaraad19@yahoo.com

Recommended Citation

Skheel Alkhafaji, Osamah Raad (2019) "The Improvement of The Solar Air Heater Duct by Wired Ribs Utilization," *Karbala International Journal of Modern Science*: Vol. 5 : Iss. 3 , Article 6.
Available at: https://doi.org/10.33640/2405-609X.1163

The Improvement of The Solar Air Heater Duct by Wired Ribs Utilization

Abstract

Abstract Heat transfer coefficient of the solar air heater duct (SAH) is low due increasing the thermal performance of its absorber. The present study tends to enhance the thermal characteristics of the SAH by adopting the wired ribs on the absorber under different ribs dimensions and arrangements. A rectangular duct is used to form the SAH with length L=1500mm, width w=100mm and height H=30mm. The used heat fluxes over the absorber are 1000W/m2 and 500W/m2 while the operated Reynolds number range is 708 ~ 6375. The utilized wired ribs are arranged over the absorber so as to develop a relative roughness height value (e/D = 0.043) in which generates a relative roughness pitch values of (P/e = 5, 10, 15). Moreover, another arrangement for the wired ribs develops a relative roughness height value (e/D = 0.086) that correspond the relative roughness pitch values of (P/e = 10, 20, 30). The results show an improvement in the average values of the Nusselt number with 9.34 % when e/D = 0.043 and heat flux of 500W/m 2 against the smooth absorber. It is also found that the average values of Nusselt number is improved with 5.31% when e/D=0.043 and heat flux = 1000W/m2.

Keywords

SAH, Ribs, Duct, Solar

1. Introduction

Solar energy is the most promised power source in the future to get on the heat energy instead of the use of common methods such as fuel burning and electric heaters. Therefore, the solar air heater (*SAH*) has considered as a recommended method for the heating purpose in the buildings by means of converting the solar energy into heat.

As a result of being that the solar energy is free cost against other types of the energy sources like oil and coal. Therefore, the enhancement of the *SAH* is required to enhance the air heating inside the buildings. The *SAH* includes a specified area in which is used to receive the solar energy where this area is known as the absorber. Moreover there are a set of roughened ribs in which are arranged on that absorber with different geometries and dimensions to improve the *SAH* performance.

The present work have the tendency to discuss the effect of using the wired ribs as turbulence generators on the absorber in which are considered to change the thermal characteristics of the *SAH*. Moreover, it tends to enlarge the study field by investigating the thermal performance under laminar and turbulent flow regions so that Reynolds number range is selected between (708−6375).

A good heat transfer rate was calculated throughout the usage of chamfered ribs over the absorber for a numerical investigation where the chamfered angle was 20° [1]. A Peak value of Nusselt number was matched at relative roughness pitch (P/e) = 6 and 12 throughout the usage of V down gaps ribs over the absorber. The enhancement of the studied work was as 3.34 times more than the smooth absorber utilization [2].

The utilized duct for [1,2] were in rectangular form where it was found that the semi-circular *SAH* was more efficient than the usage of triangular *SAH* when v ribs were used over the absorber [3]. The present study presents the effect of ribs addition on the *SAH* so an augmentation in the Nu was achieved throughout primes tic ribs on the absorber, however, this increase was conducted due to the increase air turbulences [4]. The adoption of the rectangular ribs which were inclined with 60° over the absorber of *SAH* tended to enhance heat transfer rate more than the usage of the smooth absorber [5]. The utilization of the wired ribs over the absorber with S shape arrangement was conducted an increase in the Nu under relative roughness pitch of 0.043 [6]. By adding to the previous it was found that the usage of the broken arc ribs over the absorber was led to increase in Nu by 13.8% [7]. The increase with 3.6 times in Nu was achieved due to use of v-ribs as tabulators over absorber of *SAH* where the comparisons was conducted with smooth absorber [8].

A clear enhancement in the Nusselt number was observed when the *SAH* was provided with symmetric gap and staggered gap of V-ribs. Furthermore, it was noticed that the symmetric gap and the staggered gap improved the Nusselt number with 2.3 and 2.03 respectively as a comparison to the smooth *SAH* [9]. The same type of the ribs were used to give a maximum enhancement in the Nusselt number at *P/*

Nomenclatures

A	area of the absorber
AVR	Automatic voltage regulator
Cd	Coefficient of discharge
D	Hydraulic diameter of duct
Nu	Nusselt number
g	gravitational acceleration
H	Height of solar air heater duct
h	Heat transfer coefficient
k	thermal conductivity of air
L	Length of solar air heater duct
l	Length of hot surface (absorber)
P/e	Relative roughness pitch
e/D	Relative roughness height
P	pitch distance between two ribs
m	mass flow rate of air
P	pressure
Q	Heat transfer rate
q	heat flux
SAH	Solar Air Heater
T	Temperature
w	Width of solar heater duct
W	watt

Greek symbols

ρ	air density

subscript

d	discharge
s	smooth duct, surface
f	film
∞	Environment

https://doi.org/10.33640/2405-609X.1163

$e = 10$ [10]. With By considering that the roughened ribs are the prime mover to enhance the thermal characteristics of the *SAH*. So that, the utilization of the multiple broken ribs in the *SAH* tended to make an augmentation in the heat transfer with 3.24 times than the smooth one. Moreover, the use of the square wave ribs made the enhancement in the heat transfer as 2.5 times than smooth *SAH* [11]. The summarizing of the wide studies in which were interested with the *SAH* performance had investigated by the review articles. It was found that the ribs adoption over the absorber surface has the tendency to enhance the thermal performance of the *SAH* due to breaking the laminar sublayers. The best performance was conducted when the relative roughness pitch value was 10 and the relative roughness height was 0.043 where it was noticed that the effect of the friction factor was small [12].

2. Experimental setup

An aluminum duct is designed with the dimensions of 30 mm, 100 mm and 1500 mm as height, width and length respectively. A specified area at the bottom of the duct with length of 200 mm and width of 100 mm is selected to form the absorber where this absorber acts on receiving the subjected heat fluxes throughout the testing. The heat fluxes are generated due to the utilization of an electric heater which was adopted overall the area of the absorber. The used electric heater is manufactured to provide the required amount of heat energy only without any electric shock hazards.

The variable transformer is connected the electric heater (as shown in Fig. 1) in order to change the input electric energy where this one tends to control the generated heat energy by the electric heater. Consequently, the subjected heat flux by the electric heater is modified.

K-type thermocouples are used to measure the temperature distribution overall the absorber area where these thermocouples have high response and high operation range of temperatures. It is also that the thermocouples distribution on the absorber of the *SAH* can be denoted in Fig. 3.

A digital thermocouple temperature indicator is used to read the k-type thermocouples. Each thermocouple temperature indicator is designed to receive four thermocouples at the same time consequently, this methodology is tended to use three devices of thermocouple temperature indicators. Table 1 explains the specifications of the used thermocouple temperature indicators.

A centrifugal blower is used to form a vacuum pressure inside the *SAH* where high quantity of ambient air is forced inside the duct due to the pressure difference between the duct and the ambient. The entered quantities of air is regulated by depending on speed of the blower motor where a dimmer switch is used to regulate the input voltage to the blower motor. The centrifugal blower specifications are explained in Table 2. Air flow quantity is measured by usage of a digital anemometer where this meter is made by Hold peak manufacturer and its specifications are listed in Table 3. (See Table 4).

AVR is connected between variable transformer and electric source (as shown in Fig. 1) in order to stabilize the source voltage and then prevent any fluctuation in amplitude value of the voltage.

Power meter is arranged between electric heater and variable transformer (as shown in Fig. 1) to measure the forwarded electric power and consequently measuring the supplied heat energy to the absorber. All the previous instruments are systemized by adding to the *SAH* in order to perform the required experiments as shown in Fig. 4.

The experimental procedure includes three stages where 1st stage discusses the *SAH* without ribs additive over the absorber in order to form a smooth absorber. The 2nd stage includes the addition of the wired ribs with diameter of 1 mm over the absorber, while the 3rd stage aims to replace the previous wired ribs diameter by 2 mm wired ribs. The 2nd and 3rd stages include the making of separated distances among each two ribs with 10 mm, 20 mm and 30 mm as shown in Fig. 2. Each experimental stage discusses the Nu performance heat fluxes of 500w/m^2 and 1000w/m^2 and the Reynolds number range of 708–6375. Table 4 shows all the used operated parameters such as Reynolds number values, ribs number in which are used in the present study.

3. Methodology

The results are observed by using forced heat transfer equations [2] which are listed below, so heat transfer coefficient (h) is calculated by depending on Eq. (1). The heat transfer coefficient is a function to the applied heat flux (q) and the difference between the environment and surface temperatures. The average values of measured temperatures over the absorber is denoted by the surface temperature (Ts) as explained in Eq. (2). Moreover, the average temperature between environment air temperature and the surface temperature is form the film temperature (T_f) as it is shown in Eq. (3).

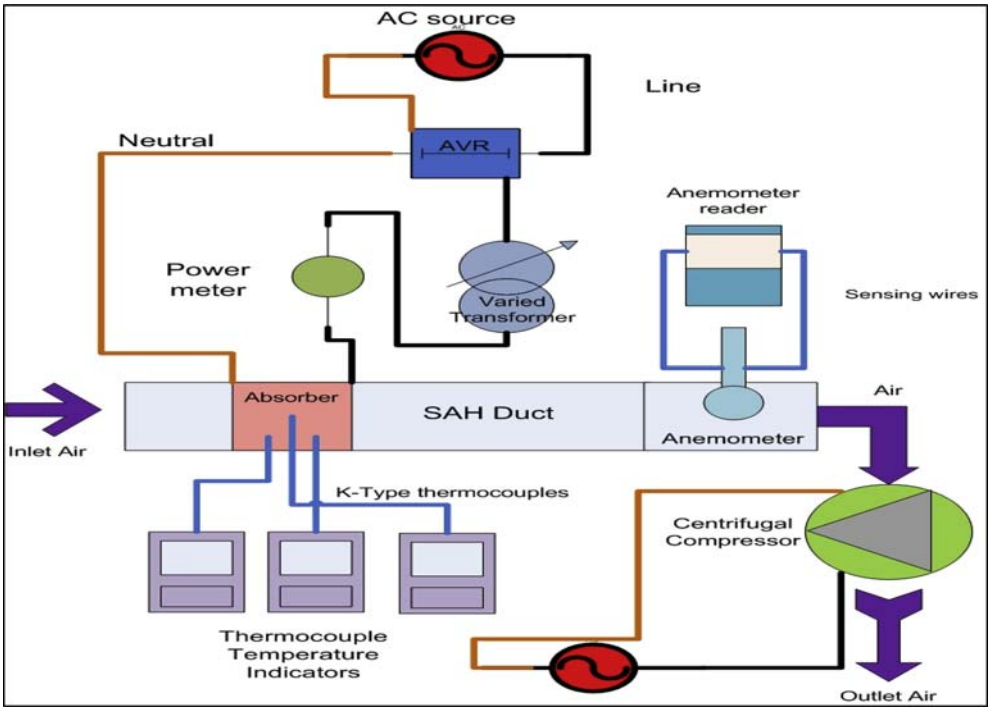

Fig. 1. A schematic diagram of the test rig.

Nu is considered as a comparative factor for predicting the increase or decrease in the heat transfer rate through the present study where *Nu* is matched by depending on Eq. (4). Adding of the wired ribs over the absorber tends to develop two parameters (*P/e* and *e/D*) where they are computed be depending on Eqs. 5 And 6 [11].

$$h = \frac{q}{Ts - T\infty} \tag{1}$$

$$Ts = \frac{\sum_1^8 T}{8} \tag{2}$$

$$Tf = \frac{T\infty + Ts}{2} \tag{3}$$

$$Nu = \frac{h.D}{k} \tag{4}$$

$$Relative\ roughness\ pitch = \frac{P}{e} \tag{5}$$

$$Relative\ roughness\ hieght = \frac{e}{D} \tag{6}$$

$$Nu(empirical) = 0.023Re^{0.8}Pr^{0.4} \tag{7}$$

4. Validation

In order to get on the accuracy of the present experimental study so that a validation are done for this

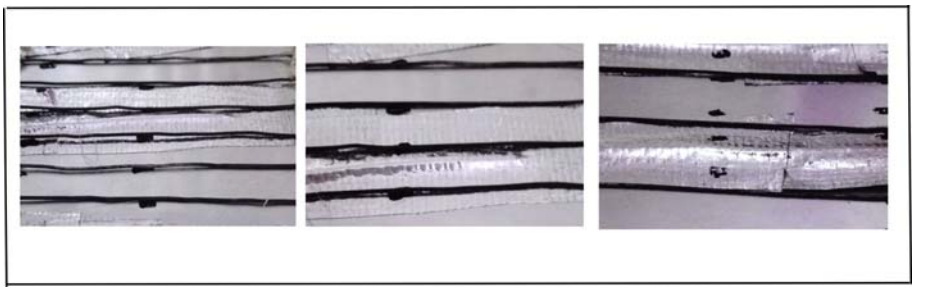

Fig. 2. Separated distances among circular wired ribs.

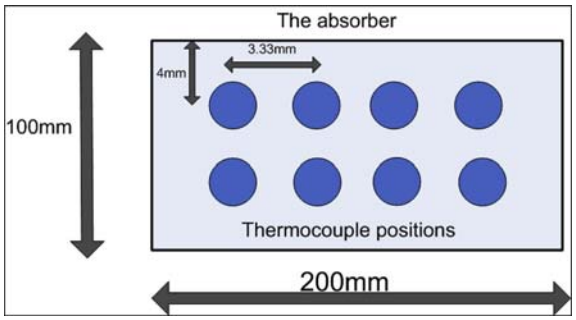

Fig. 3. Thermocouple positions on the absorber of SAH.

purpose. The empirical equation of the Dittus Boilter (Eq. (7)) has been depended by comparing the calculated results with the experimental results for the smooth *SAH*. The values of the empirical equation have a deviation with ±3.21% as a comparison to the experimental results as it shown in Fig. 5.

5. Results and discussion

5.1. Nu and Re

Figs. 6 and 7 refers to the increase in Nu by increasing Re for different *P/e* and *e/D*. This is because of the reduction in the thermal sub layers over the absorber where this reduction is because of the air flow increasing that tends to increase the turbulences. Consequently, the reduction in thermal sub layers tends to reduce the thermal resistance over the absorber and increase the heat transfer by convection between absorber and the air. It is important to know that the increase in the relative roughness pitch from 0.043 to 0.086 are considered in order to increase the tendency of turbulences occurrence to eliminate the thermal sub-layers. This increase acts on extending the ribs beyond the laminar sub-layer the order that causes a disturbance for the flow.

It is observed that the increase in Nu is associated with the increase of *P/e* values for both Figs. 6 and 7 [10]. The great values of *P/e* mean a reducing in the number of the wired ribs over the absorber and this lead to increase the area between each two ribs. The increase of that area tends to enhance the heat transfer by convection due to increasing the convection area which is always being in touch with the air. Consequently, *Nu* values are noticed highly by increasing the values of *P/e*.

It is important to notice that although of being the area of absorber is more in smooth absorber (absorber without ribs) but the turbulence intensity of flow may be low because of the wired ribs missing. However, the absorber without wired ribs depends on the increase in Re to activate the turbulences of air.

It is noticed that the mean values of Nu when $e/D = 0.043$ is more greatly as compared to that mean values of Nu at $e/D = 0.086$. This performance gives an indication that the usage of *SAH* gives best thermal performance at $e/D = 0.043$ more than $e/D = 0.086$. It is also gives an indication that the height of ribs does not play an effective role to enhance the thermal performance of the *SAH*.

Figs. 8 and 9 present the same as trend behavior between *Nu* and *Re* where the increase of the values of *Nu* are joint with the increase of the *Re* values. Fig. 8 shows highly values for the Nu at $P/e = 10$ while the lower values of *Nu* are noticed for $P/e = 30, 20$. This is because of the higher thermal resistance which is generated due to the high heat flux (1000 W/m^2) that is subjected to the absorber.

The lower values of the *P/e* mean a lot of the wired ribs which are arranged over the absorber where this one leads to increase the turbulences of air. The increase in *P/e* values mean a reduction in the number of ribs and this make a reduction in the turbulences

Table 1
Thermocouple thermometer specifications.

No	Item
1	Temperature range = −200 °C~1372 °C
2	Accuracy = ±0.1 °C < 100 °C
3	Resolution = 1 °C < 1000 °C
4	Weight = 230 gm
5	Input thermocouples = K-type
6	Thermocouples number = 4 channel
7	Power source = 9v battery

Table 2
Centrifugal blower specifications.

No	Item
1	Vacuum pressure >19Kpa
2	Operation voltage = 220v ~240v
3	Power = 1200 w

Table 3
Anemometer specifications.

No	Item
1	Resolution = 0.1
2	Operation range = 0–30 m/s
3	Air temperature range = −10°~45 °C
4	Accuracy = ±5%
5	Weight = 320 gm
6	Power source = 9v battery

Table 4
The observation table.

Absorber status	Ribs number	Ribs diameter (mm)	P/e	e/D	Applied heat (W)	Reynolds No. range
Smooth	0	0	0	0	500	708–6375
Roughened	18	1	10	0.043	500	708–6375
Roughened	8	1	20	0.043	500	708–6375
Roughened	6	1	30	0.043	500	708–6375
Smooth	0	0	0	0	1000	708–6375
Roughened	18	2	5	0.086	1000	708–6375
Roughened	8	2	10	0.086	1000	708–6375
Roughened	6	2	15	0.086	1000	708–6375

Fig. 4. The experimental set-up.

effectivity of the flowing air. Therefore, Fig. 9 has highly values of Nu at $P/e = 10$ because of the effectiveness of air turbulences which tend to eliminate the thermal sublayers over the absorber. It is also noticed that the lower values of Nu are matched when the values of $P/e = 30, 20$ where this is due to the thermal sublayer poor elimination at these cases.

This behavior does not show in Fig. 9 so the greatly values of the Nu are joint with increasing the values of

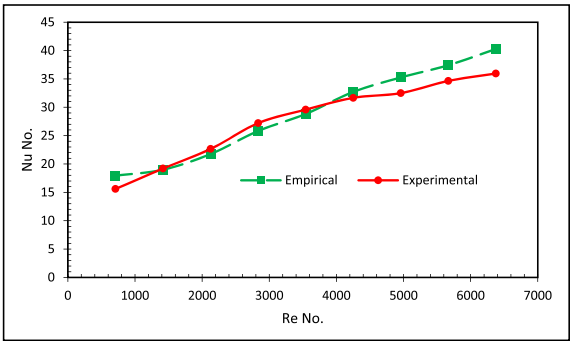

Fig. 5. Nusselt number for empirical and experimental states at heat flux of 500 W/m.^{2}.

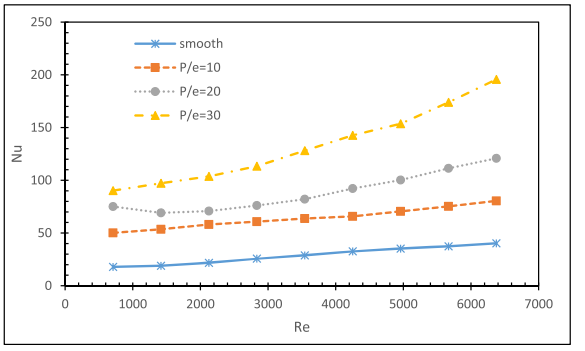

Fig. 6. Re and Nu at 500 W/m^2 and e/D = 0.043.

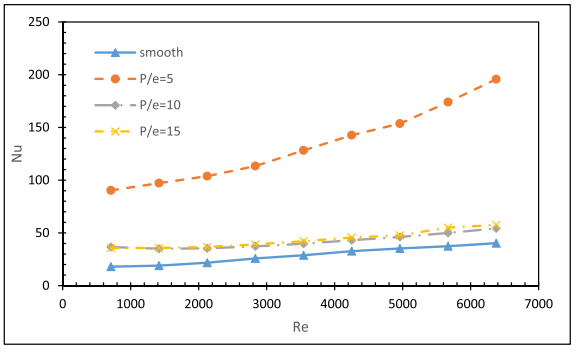

Fig. 7. Re and Nu at 500 W/m^2 and e/D = 0.086.

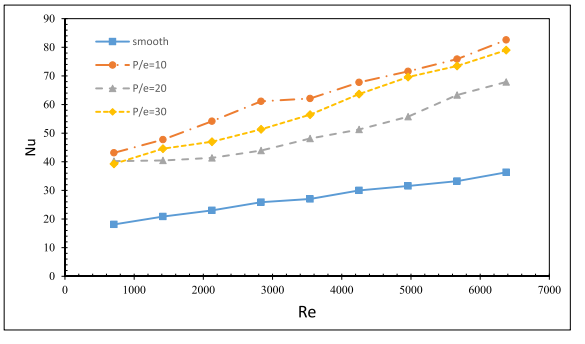

Fig. 8. Re and Nu at 1000 W/m^2 and e/D = 0.043.

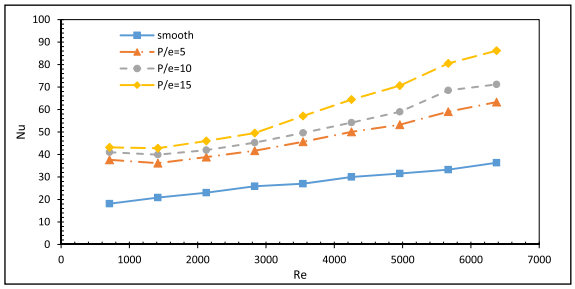

Fig. 9. Re and Nu at 1000 W/m^2 and e/D = 0.086.

P/e. This is because of increasing the value of *e/D* (*e/D* = 0.086) which refers to the increase in the value of the wired rib height so this one enhance the air turbulences as much as possible.

6. Conclusions

In the present study, the *SAH* has been tested under the utilization of the wired ribs over the absorber. The used rib diameters are 1 mm and 2 mm so this one leads to make the values of relative roughness pitch *P/e* and relative roughness height *e/D* are (5, 10, 15, 20, 30) and (0.043, 0.086) respectively. The experimental procedure includes the testing of *SAH* under a wide range of the *Re* in order to cover Laminar and turbulent flow regions. The used air has been accelerated with different velocities to get on the required range of the *Re* (708–6375). The harvested results have been processed by depending on the heat transfer relations in order to estimate the performance of the tested *SAH* and they are:

1 The increase in the values of *Re* provide highly values for the *Nu* for all the experimental cases.
2 The thermal performance of the *SAH* is enhanced by the addition of the wired ribs over the absorber.
3 The best thermal performance is achieved for the *SAH* at *P/e* = 30 and *e/D* = 0.043 where these values are matched at the use of the rib diameter = 1 mm.
4 The enhancement in the mean values of Nu at the usage of *e/D* = 0.043 and *e/D* = 0.086 are 9.34% and 4.05% respectively where these values are conducted with the comparison to the smooth absorber and heat flux = 500 W/m^2.
5 The enhancement of the average values of the Nu at the utilization of *e/D* = 0.043 and *e/D* = 0.086 are 5.31% and 4.79% respectively where these values are conducted with the comparison to the smooth absorber and heat flux = 1000 W/m^2.

These percentage values indicated that the value of *e/D* which equal to 0.043 provides good performance for the *SAH* when the heat flux is 500 W/m^2. Moreover, the used value of *e/D* = 0.086 is more suitable for the *SAH* when the heat flux is 1000 W/m^2.

Appendix. Uncertainty Analysis

Any experimental work is affected with the accuracy of the measurement devices and the response time of extracting the results. Therefore, multi computation procedures should be followed to check the generated errors during tests. Kline and McClintock method has been used to predict that values of uncertainty [13]. This method depends on the governed equation of such discussed parameter, where the equation of Nusselt number depends on heat transfer coefficient, thermal conductivity of air and the hydraulic diameter of the duct. So that, the error deviation of each parameter in the Nusselt number equation should be known then it should be processed by Eq. (A.1) as shown below to get on the uncertainty of the Nusselt number factor.

If the governed equation of such parameter (*U*) is *U* = *R.S* then:

$$\frac{\partial U}{U} = \sqrt{\left(\frac{\partial R}{R}\right)^2 + \left(\frac{\partial S}{S}\right)^2} \qquad (A.1)$$

The main discussed parameters in the present study are Nusselt number, Reynolds number and the measured dimensions such as hydraulic diameter and the area of the absorber.

Table A.1
The uncertainty of the used instruments

Instrument	Uncertainty
Thermocouple temperature indicator	±0.1C
Anemometer	±0.05 m/s
Power meter (watt meter)	±0.01 W
Vernier clipper	±1 mm
Portable Barometer	±1.5 kpa

Table A.2
The values of the measured parameters

Parameter	Value
Length of absorber	200 mm
Width of absorber	100 mm
Atmospheric pressure	110kpa
Hydraulic diameter of duct	23 mm
Maximum applied power to the absorber	1000 W
Temperature of the Lab.	32.8C
Maximum surface temperature	46.7C

1 The uncertainty of area of the absorber (A = l.w)

$$\frac{\partial A}{A}=\sqrt{\left(\frac{\partial l}{l}\right)^2+\left(\frac{\partial w}{w}\right)^2}=\sqrt{\left(\frac{1}{200}\right)^2+\left(\frac{1}{100}\right)^2}=0.0206$$

2 uncertanty of the air density $\left(\rho=\frac{P}{RT}\right)$

$$\frac{\partial \rho}{\rho}=\sqrt{\left(\frac{\partial P}{P}\right)^2+\left(\frac{\partial T}{T}\right)^2}=\sqrt{\left(\frac{1.5}{110}\right)^2+\left(\frac{0.1}{32.8}\right)^2}=0.013$$

3 uncertanity of thermal conductivity of the air $k = 0.0257 *(T_f/293)^{0.86}$ [13]

$$\frac{\partial k}{k}=\sqrt{\left(\frac{\partial Tf}{Tf}\right)^2}=\sqrt{\left(\frac{0.1}{32.8}\right)^2}=0.0033$$

4 uncertainty of the kinematic viscosity of air ($\mu = 1.81*10^{-5}*(Tf/293)^{0.735}$) [13].

$$\frac{\partial \mu}{\mu}=\sqrt{\left(\frac{\partial Tf}{Tf}\right)^2}=\sqrt{\left(\frac{0.1}{32.8}\right)^2}=0.0033$$

5 uncertanity of the air velocity inside the *SAH*

$$\frac{\partial V}{V}=\sqrt{\left(\frac{\partial V}{V}\right)^2}=\sqrt{\left(\frac{0.05}{15}\right)^2}=0.003$$

6 uncertanity of the Reynolds number

$$\frac{\partial Re}{Re}=\sqrt{\left(\frac{\partial \rho}{\rho}\right)^2+\left(\frac{\partial V}{V}\right)^2+\left(\frac{\partial Dh}{Dh}\right)^2+\left(\frac{\partial \mu}{\mu}\right)^2}$$

$$\frac{\partial Re}{Re}=\sqrt{(0.013)^2+(0.003)^2+\left(\frac{1}{230}\right)^2+(0.0033)^2}=0.066$$

6 uncertanity of the heat transfer coefficient (h = q/(Ts-Tf)) [14].

$$\frac{\partial h}{h}=\sqrt{\left(\frac{\partial q}{q}\right)^2+\left(\frac{\partial Tf}{Tf}\right)^2+\left(\frac{\partial Ts}{Ts}\right)^2}$$

$$\frac{\partial h}{h}=\sqrt{\left(\frac{0.01}{1000}\right)^2+\left(\frac{0.1}{32.8}\right)^2+\left(\frac{0.1}{46.7}\right)^2}=0.0037$$

7 uncertanity of the Nusselt number

$$\frac{\partial Nu}{Nu}=\sqrt{\left(\frac{\partial h}{h}\right)^2+\left(\frac{\partial Dh}{Dh}\right)^2+\left(\frac{\partial k}{k}\right)^2}$$

$$\frac{\partial Nu}{Nu}=\sqrt{(0.0037)^2+\left(\frac{1}{230}\right)^2+(0.0033)^2}=0.003$$

References

[1] Vipin B. Gawande, A.S. Dhoblea, D.B. Zodpea, Sunil Chamolib, Analytical approach for evaluation of thermo hydraulic performance of roughened solar air heater, Case Stud. Therm. J.Eng. 8 (September 2016) 19–31.

[2] Narinderpal Singh Deo, Subhash Chander, J.S. Saini, Performance analysis of solar air heater duct roughened with multi gap V-down ribs combined with staggered ribs, Renew. Energy 91 (2016) 484e500.

[3] Satyender Singh, Thermal performance analysis of semicircular and triangular cross-sectioned duct solar air heaters under external recycle, J Energy Storage 20 (2018) 316–336.

[4] Naveen Sharma, Andallib Tariq, Manish Mishra, Detailed heat transfer and fluid flow investigation in a rectangular duct with truncated prismatic ribs, Exp. Therm. Fluid Sci. 96 (September) (2018) 383–396.

[5] Linqi Shui, Jianmin Gao, Xiaojun Shi, Jiazeng Liu, Effect of duct aspect ratio on heat transfer and friction in steam-cooled ducts with 60° angled rib tabulators, Exp. Therm. Fluid Sci. 49 (September) (2013) 123−134.

[6] Khushmeet Kumar, D.R. Prajapati, Sushant Samir, Heat transfer and friction factor correlations development for solar air heater duct artificially roughened with 'S' shape ribs, Exp. Therm. Fluid Sci. 82 (April) (2017) 249−261.

[7] V.S. Hans, R.S. Gill, Sukhmeet Singh, Heat transfer and friction factor correlations for a solar air heater duct roughened artificially with broken arc ribs, Exp. Therm. Fluid Sci. 80 (January) (2017) 77−89.

[8] Rajesh Maithani, J.S. Saini, Heat transfer and friction factor correlations for a solar air heater duct roughened artificially with V-ribs with symmetrical gaps, Exp. Therm. Fluid Sci. 70 (January) (2016) 220−227.

[9] Piyush Kumar Jain, Atul Lanjewar, Over View of V-Rib Geometries in Solar Air Heater and Performance Evaluation of a New V-Rib Geometry, Renewable Energy (2018), https://doi.org/10.1016/j.renene.2018.10.001.

[10] Sumer Singh Patel, Atul Lanjewar, Experimental and numerical investigation of solar air heater with novel V rib Geometry, J Energy Storage 21 (2019) 750−764.

[11] Rajneesh Kumar, Anoop Kumar, Varun Goel, A parametric analysis of rectangular rib roughened triangular duct solar air heater using computational fluid dynamics, Sol. Energy 157 (2017) 1095−1107.

[12] Inderjeet Singh, Sukhmeet Singh, A review of artificial roughness geometries employed in solar air heaters, Renew. Sustain. Energy Rev. 92 (2018) 405−425.

[13] Inderjeet Singh, Sachit Vardhan, Sukhmeet Singh, Amritpal Singh, Experimental and CFD analysis of solar air heater duct roughened with multiple broken transverse ribs: a comparative study, Sol. Energy 188 (2019) 519−532.

[14] A. Yunus, Cengel "Heat and Mass Transfer Fundamentals and Applications, second ed., Mcgraw hill, 2014.